8

THERMAL BUCKLING OF ANTI-SYMMETRIC COMPOSITE PLATES WITH GEOMETRIC NON-LINEARITY USING FINITE ELEMENT METHOD

Z. A. Rasid
N. Abdullah N. Mohamad

8.0 INTRODUCTION

Fibre reinforced composite (FRC) is an important material to be considered in the design of structures that require high strength to weight ratio. Examples of these structures are high performance aerospace vehicles such as high speed aircrafts, rockets and launch vehicles. To enhance this property of high strength to weight ration, FRC components are usually made thin and curvy. As a result, one important mode of failure to be considered in these FRC component designs is buckling failure which can be due to compressive mechanical or thermal loading. For the mentioned high performance aerospace vehicles, thermal loading is unavoidable. Thermal loading here is caused by aerodynamic heating which is due to the supersonic or hypersonic flight. This heating will provide the structure's external skin with thermal compressive load since the inner part of the skin remains cooler and thus restrains the free expansion of the skin. Consequently the outer skin will be subjected to thermal buckling because of the mentioned typical low thickness in the FRC components [1]. It is

well known that thermal buckling of plate structures is a sudden huge lateral deflection that occurs when the temperature of the plates increases above the critical temperature, T_{cr}. It is also known that buckling in a plate structure is not a snap-through type that can result in a total collapse of the structure. It is rather of a huge deflection of the plate that requires attention on how much can the plate withstands further loading after buckling occurs. The understanding of the post-buckling behaviour that occurs after the occurrence of critical buckling is thus important in maximizing the usage of the structures. The determination of these patterns of behaviours of thermal post-buckling of laminated composite plates is the objective of this study.

Thermal buckling of laminated composite plates was studied using the finite element method by Prabhu, M.R. and Dhanaraj, R [2]. The parametric studies of the thermal buckling analysis on the symmetric angle-ply and cross-ply and the quassi-isotropic laminates were conducted. The influence of the stress distribution on the variation of critical temperature with fibre orientation was studied for different boundary conditions. It was found among others that the variation of T_{cr} is not symmetric with respect to $\theta = 45^0$ for symmetric angle-ply laminates. A similar study was conducted by Shankara, C.A. and Iyengar, N.G.R [3]. They however used both the higher order shear deformation theory (HSDT) and the FSDT of composites to describe the kinematics of the composites. As a result, similar findings to the studies conducted by [2] were obtained. Chen et al [4] enhanced the studies on thermal buckling of composite plates by considering the non-uniform temperature distribution. It was found that the effects of lamination angle, modulus ratio, plate aspect ratio and boundary conditions upon the critical temperatures were significant. Studies on thermal post-buckling of laminated composite plates using the FEM were conducted by Singh, G. and Rao, G.V. [5]. They used the nonlinear strain-displacement relations, which include thermal strains and allow parabolic variation of transverse shear strain with vanishing of transverse shear stress at the top and bottom surfaces of the plates. A sequence of linear eigen-value problems was

solved to trace the thermal buckling path of symmetric angle-ply plates. The investigation revealed that the post-buckling path may not remain stable throughout. It was shown that secondary instabilities did take place from the post-buckling path. Averill and Reddy [6] conducted geometrically nonlinear analysis to compare the effect of transverse normal deformation in the FSDT and the HSDT on the thermal buckling responses of composite structures. It was found that if the transverse normal deformation was constrained, the thermal buckling responses predicted by the FSDT were completely different from the responses predicted by the HSDT. Singha, M.K. et. al [7] extended the study of [5] by considering the temperature dependent properties of laminated composite plates. The analysis revealed that there exist two thermal instabilities in the composite plates.

In this study, the total Lagrangian approach of the Newton Raphson scheme is used to trace the thermal post-buckling paths of anti-symmetric angle-ply laminated composites. The FSDT of composites with the added von Karman's nonlinear moderate strain terms was used to describe the kinematics of the composites. Combining these strain equations, the constitutive equations of the laminated composite and the principle of virtual work equations has resulted in the finite element governing non-linear equations that represent the buckling and post-buckling behaviour of laminated composite plates. The source codes were developed to solve these governing non-linear equations. With this model, studies were conducted on the anti-symmetric angle-ply laminated composite plates. Several parameters that affect the thermal post-buckling behaviour of laminated composite plates such as the numbers of layers, aspect ratios, side to thickness ratios and boundary conditions of the plates were studied. It is hoped that these studies on the important thermal post-buckling behaviour of laminated composite plates using the developed model can improve the current state of understanding on the subject and thus become useful in the design of aerospace vehicles.

8.1 MODELLING OF COMPOSITE PLATES FOR THERMAL POST-BUCKLING PROBLEMS

The laminated composite plates to be modelled here are such as shown in Figure 8.1. The xyz- coordinate system is the Cartesian coordinate system while the 123 – coordinate system is the material coordinate system. a and b are the side length of the plate while h is the total thickness of the plate. The in-plane constitutive relationship that includes the temperature effect for a composite plate in the material coordinate system is well known to be

$$\begin{Bmatrix} \sigma_1 \\ \sigma_2 \\ \sigma_{12} \end{Bmatrix} = \begin{bmatrix} Q_{11} & Q_{12} & 0 \\ Q_{12} & Q_{22} & 0 \\ 0 & 0 & Q_{33} \end{bmatrix} \left\{ \begin{Bmatrix} \varepsilon_1 \\ \varepsilon_2 \\ \gamma_{12} \end{Bmatrix} - \begin{Bmatrix} \alpha 1 \\ \alpha_2 \\ 0 \end{Bmatrix} \Delta T \right\} \tag{1a}$$

or in a short form,

$$\{\sigma_1\} = [Q]\{\varepsilon_1\} - \{\alpha_1\}\Delta T \tag{1}$$

where $[Q]$ is the reduced stiffness matrix of the composite [8] and $\{\sigma_1\}$, $\{\varepsilon_1\}$ and $\{\alpha_1\}$ are the vectors of stress, strain and thermal coefficient of expansion in the material coordinate system.

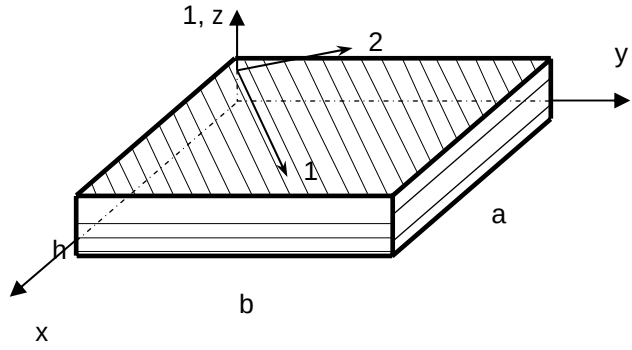

Figure 8.1. The laminated composite plate

For the transverse constitutive relationship, refer to [8]. Using the transformation matrix [8] we have,

$$\{\sigma_x\} = \left[\overline{Q}\right]\{\varepsilon_x\} + \{\alpha_x\}\Delta T \tag{2}$$

where $[\overline{Q}]$ is the transformed reduced stiffness matrix of the composites, and $\{\sigma_x\}$, $\{\varepsilon_x\}$ and $\{\alpha_x\}$ are the vectors of stress, strain and thermal coefficient of expansion in the Cartesian coordinate system (x-y-z). Using the Mindlin's FSDT [9], displacements at any points in laminated composite plates can be expressed as,

$$\begin{aligned} u(x,y,z,t) &= u_o(x,y,t) + z\,\theta_x(x,y,t) \\ v(x,y,z,t) &= v_o(x,y,t) + z\,\theta_y(x,y,t) \\ w(x,y,z,t) &= w_o(x,y,t) \end{aligned} \tag{3}$$

where u_o, v_o and w_o are the mid-plane displacements in the x, y and z directions respectively while θ_x and θ_y are the normal rotations in the xz-plane and yz-plane respectively and t is the time variable. By including the von Karman's strain, the strain can be expressed as

$$\{\varepsilon\} = \begin{Bmatrix} \varepsilon_{xx} \\ \varepsilon_{yy} \\ \gamma_{xy} \end{Bmatrix} = \begin{Bmatrix} \frac{\partial u}{\partial x} \\ \frac{\partial v}{\partial y} \\ \frac{\partial u}{\partial y} + \frac{\partial v}{\partial x} \end{Bmatrix} + \frac{1}{2}\begin{Bmatrix} \left(\frac{\partial w}{\partial x}\right)^2 \\ \left(\frac{\partial w}{\partial y}\right)^2 \\ 2\left(\frac{\partial w}{\partial x}\right)\left(\frac{\partial w}{\partial y}\right) \end{Bmatrix} + z\begin{Bmatrix} \frac{\partial \theta_x}{\partial x} \\ \frac{\partial \theta_y}{\partial y} \\ \left(\frac{\partial \theta_x}{\partial y} + \frac{\partial \theta_y}{\partial x}\right) \end{Bmatrix} \tag{4}$$

or

$$\begin{aligned} \{\varepsilon\} &= \{\varepsilon_p\} + z\{\kappa\} \\ &= \{\varepsilon_m\} + \{\varepsilon_{nl}\} + z\{\kappa\} \end{aligned} \tag{5}$$

where $\{\varepsilon_m\}$, $\{\varepsilon_{nl}\}$ and $\{\kappa\}$ are the in-plane linear strain vector, the in-plane nonlinear strain vector and the curvature strain vector, respectively. The transverse shear strain vector is as the following

$$\{\gamma\} = \begin{Bmatrix} \gamma_{xz} \\ \gamma_{yz} \end{Bmatrix} = \begin{Bmatrix} \dfrac{\partial w}{\partial x} + \theta_y \\ \dfrac{\partial w}{\partial y} + \theta_y \end{Bmatrix} \tag{6}$$

Defining stress resultants in the usual ways [9] for the laminated composite, we have constitutive relationship regarding the in-plane stress

$$\begin{Bmatrix} \{N\} \\ \{M\} \end{Bmatrix} = \begin{bmatrix} [A] & [B] \\ [B] & [D] \end{bmatrix} \left(\begin{Bmatrix} \{\varepsilon_m\} \\ \{\kappa\} \end{Bmatrix} + \begin{Bmatrix} \{\varepsilon_{nl}\} \\ 0 \end{Bmatrix} \right) + \begin{Bmatrix} \{N_T\} \\ \{M_T\} \end{Bmatrix} \tag{7a}$$

and for the out of plane stress,

$$\{Q\} = \begin{Bmatrix} Q_{xz} \\ Q_{yz} \end{Bmatrix} = \begin{bmatrix} A_{44} & A_{45} \\ A_{45} & A_{55} \end{bmatrix} \{\gamma\} = [A'] \{\gamma\} \tag{7b}$$

where [*A*], [*B*], [*D*] and [*A'*] are the laminate material matrices while {*N*} and {*M*} are the force and moment resultant vectors, respectively. {N_T} and {M_T} are the resultant force and moment vectors due to the change in temperature respectively such as

$$(\{N_T\}, \{M_T\}) = \sum_{k=1}^{n} \int_{-\frac{t}{2}}^{\frac{t}{2}} [\overline{Q}] \{\alpha_x\} \Delta T(1, z) dz \tag{7c}$$

Applying the finite element method, eight noded isoparametric quadrilateral elements are used here. Each node carries 5 degrees of freedom.

$$\{a\} = [N]\{q\} \tag{8a}$$

$$\{q\}^T = \{u_1, v_1, w_1, \theta x_1, \theta_{y1}, u_2, .. , w_8, \theta x_8, \theta_{y8}\} \tag{8b}$$

where {*a*} and {*q*} are the generalised and nodal displacement vectors and [*N*] is the shape function matrix. The principle of virtual works can be stated as

$$\delta W = \delta W_{int} - \delta W_{ext} = 0 \tag{9a}$$

$$\delta W_{int} = \{\delta q\}^T \int_A \{\delta\varepsilon_m\}^T \{N\} + \{\delta\varepsilon_{nl}\}^T \{N\} + \{\varepsilon_b\}^T \{M\} + \{\varepsilon_s\}^T \{Q\} dA \tag{9b}$$

Inseting equations (5)-(8b) into (9b) and following the standard FEM modelling procedures [8], we have

$$\delta W_{int} = \{\delta q\}^T \left([K_L] + [K_s] - [K_T] + [K_G] + \frac{1}{2}[N1] + \frac{1}{3}[N2] \right) \{q\} - \{\delta q\}^T \{P_T\} \quad (10)$$

Since there are no external loads,

$$\delta W_{ext} = 0 \quad (11)$$

Inserting equations (10) and (11) into equation (9a), the FEM governing equation for the geometric nonlinear buckling problem of composite plates can be obtained as in the following.

$$\left([K_L] + [K_s] - [K_T] + [K_G] + \frac{1}{2}[N1] + \frac{1}{3}[N2] \right) \{q\} = \{P_T\} \quad (12)$$

where $[K_L]$, $[K_s]$, $[K_G]$ and $[K_T]$ are the linear, shear, geometric and thermal stiffness matrices and $[N_1]$and $[N_2]$ are the first and second order nonlinear stiffness matrices. Equation (12) is a nonlinear equation. One way to solve this equation is by using the Newton Raphson's scheme and here the total Lagrangian approach is used. Introducing a function of residual forces, $\{\psi\}$.

$$\{\psi(q)\} = \left([K_L] + [K_s] - [K_T] + [K_G] + \frac{1}{2}[N1] + \frac{1}{3}[N2] \right) \{q\} - \{P_T\} \quad (13)$$

Due to the Taylor's approximation [8],

$$\psi(q)^{n+1} = \psi(q)^n + \left(\frac{d\psi}{dq} \right)_n \{\delta q\}^n + \text{Higher order terms} \quad (14)$$

where

$$\left(\frac{d\psi}{dq} \right)_n = [K_{\tan}]_n = \left([K_L] + [K_s] - [K_T] + [K_G] + [N_1] + [N_2] \right)_n \quad (15)$$

so that

$$[K_{\tan}] \{\delta q\}^n = -\varphi(q)^n \quad (16)$$

and displacements are incremented such as

$$\{q\}^{n+1} = \{q\}^n + \{\delta q\}^n \quad (17)$$

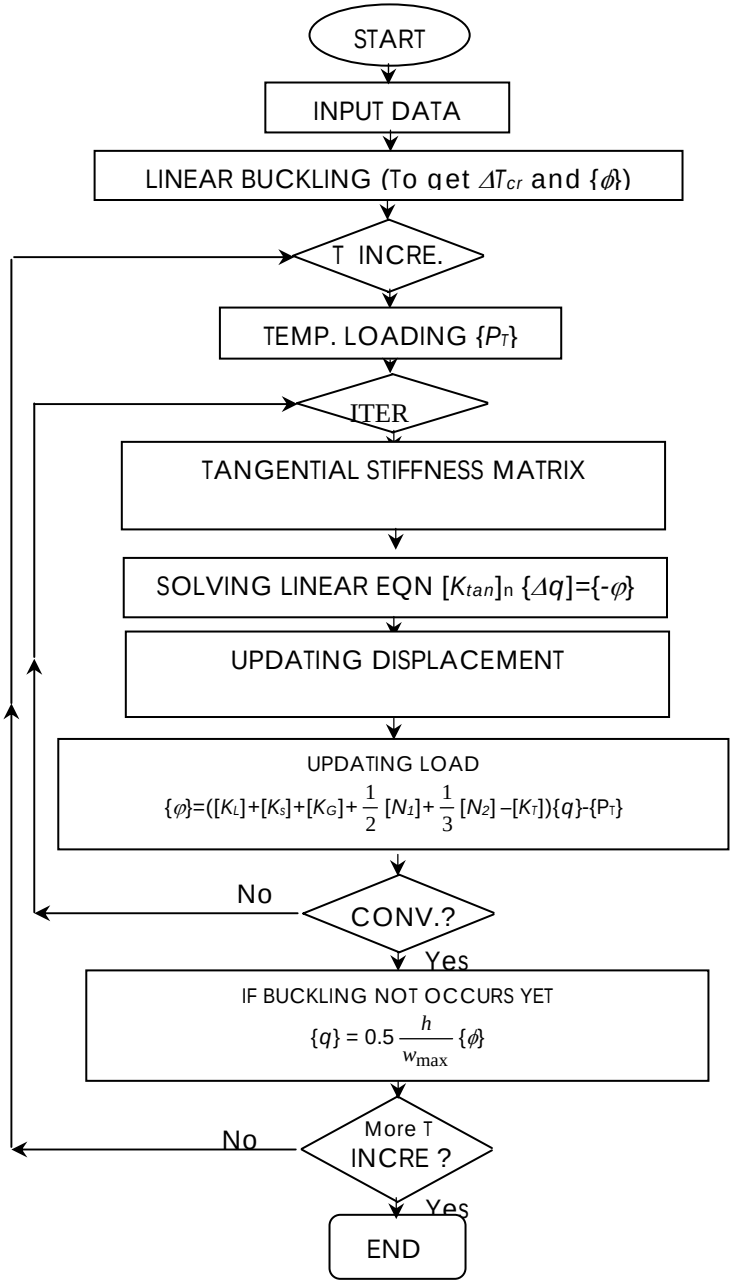

Figure 8.2: Flow-chart for the development of the source codes

FEM source codes for solving equations (15)-(17) were developed. To detect the bifurcation point, linear thermal buckling was conducted initially on the composite plates. By this process, the critical temperature, ΔT_{cr} and its associated eigen-vector, $\{\phi\}$ can be determined. The eigen-vector was used as the initial trial value of the initial transverse displacement. The initial displacement vector is set to be

$$\{q\} = 0.5\frac{h}{w_{\max}}\{\phi\} \tag{18}$$

for each increment of temperature until a significant value of displacement can be achieved which means that the post-buckling has occurred. $\{q\}$ here is the vector of generalised displacement and h is the total thickness of plates. The flow-chart of this algorithm is shown in Figure 8.2. Following this, the results of the post-buckling of SMA composite plates are given next.

8.2 RESULTS AND DISCUSSIONS

The effects of several parameters on post-buckling behaviours of composite plate are studied for anti-symmetric angle-ply composite plates. The angle of orientation for most cases is $[45/-45]_2$. Referring to Figure 8.1, the aspect ratio, a/b is 1.0 with a=b=0.1m and the side to thickness ratio, a/h is 100 unless specified differently. Two typical mechanical properties of graphite- epoxy composites are used here:

Property 1 (P1):
E_1= 155.0E9, E_2= 8.07E9, v_{12}= 0.22, G_{12}= 4.55E9, G_{23}= 4.55E9, G_{13}=3.25E9, α_1= -0.07E-6, α_2= α_3= 30.1E-6

Property 2 (P2):
E_1/E_2=40, E_2=6.25, G_{12}/E_2=0.8, G_{12}=G_{13}, G_{23}/E_2=0.52, v_{12}=0.24, α_2/α_1=10.
In most cases, the hinged boundary condition (HH) is used. However as for comparison, the boundary conditions of simply

supported (SS) and clamped (CC) at all edges are applied too. The conditions for these three boundary conditions are shown below.

HH - at x=0, a : $u=v=w=\theta_y=0$, at y=0, b : $u=v=w=\theta_x=0$
S S - at x=0, a : $u=w=\theta_y=0$, at y=0, b : $v=w=\theta_x=0$
CC - at x=0, and y=0, b : $u=v=w=\theta_x=\theta_y=0$

8.2.1. Validation

Convergence tests are conducted for the linear thermal buckling analysis. Three composite configurations are used: $[30/30]_2$, $[30]30]_s$ and $[0/90]_2$. The P2 property is used here. Table 8.1 shows that the results from the current analysis are in good agreement with the results available from the literature. It was decided to use the 6x6 elements in this study.

Table 8.1: Convergence test for the linear thermal buckling analysis

	[8]	4x4	5x5	6x6	8x8
$(30/-30)_s$	8.396	9.200	8.735	8.580	8.431
$(30/30)_2$	10.169	10.210	10.178	10.168	10.162
$(0/90)_2$	21.166	24.468	22.219	21.743	21.570

Post-buckling analysis was conducted on a qussi-isotropic and an orthotropic plates. In the former analysis, the composite configuration is $[45/-45/0/90]_s$. The plate is 0.15m x 0.15m with the length to thickness ratio, a/h = 150. The P1 property is used here. In the latter case, the configuration of the composite plate is $[45/-45]_2$ and the P2 property is used. The plate is 0.1m x 0.1m with the length to thickness ratio, a/h=100. Figure 8.3 and 8.4 show that the results of the two analyses agree excellently to the finding of the past literatures.

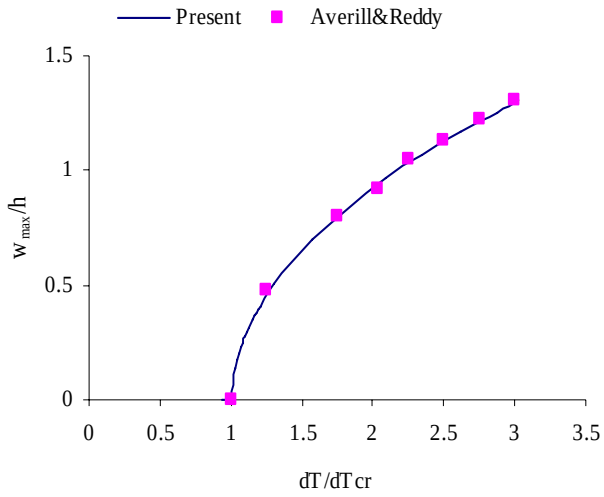

Figure 8.3. The thermal post-buckling of a quassi-isotropic plate

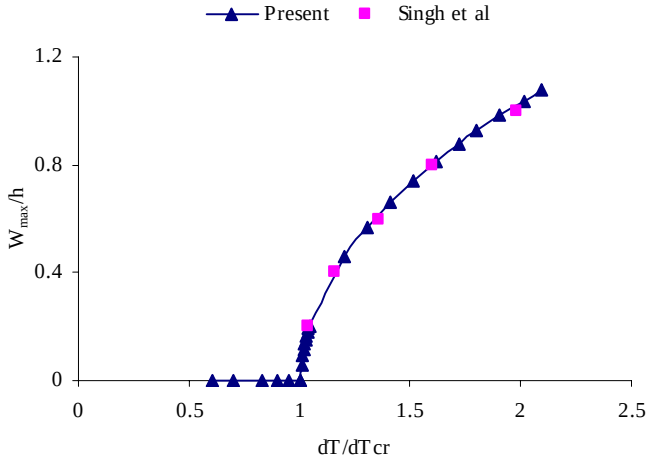

Figure 8.4. The thermal post-buckling of anti-symmetric angle-ply composite plate

8.2.2. The effect of the number of layers

This study is conducted on composite configuration of $[45/-45]_n$ where n represents the number of layers of the composites. Material property of P1 is used here. The total thickness of the composites remains the same as the numbers of layers are increased. Figure 8.5 shows that in all cases, buckling starts to occur at ΔT_{cr} values as were predicted by the linear buckling analysis. Critical thermal buckling loads (λ_n) increased as the numbers of layers are increased. The post-buckling paths are stable throughout the range of applied ΔT. Figure 8.5 also shows that as the number of layers is increased from four to six, the ratios of $\frac{\Delta T}{\Delta T_{cr}}$ decreased for the same amount of lateral deflection. However this decreasing trend reduced as more layers are increased. The reason for this is the well known existence of the composite property where as the number of layers is increased, the bending-extensional coupling effects of the laminated composite that contributes to this trend decreased at the same time.

8.2.3. The effect of the plate thickness

In this study, the thickness of plates, h are changed for the same amount of side length, a=0.1m. The plates with configuration $[45/-45]_2$ and P1 material property are used here. As expected, Figure 8.6 indicates that the critical loads decreased as the thickness is decreased. However, Figure 8.6 also shows that similar to the previous study of the effect of the number of layers on the post-buckling of plates, the ratios of $\frac{\Delta T}{\Delta T_{cr}}$ decreased as the ratios $\frac{a}{h}$ are increased. As such, the same reason is applied here where, as the number of layers is increased, the bending-extensional coupling effect of the laminated composite that contributes to this trend decreased at the same time. In all cases, buckling can be seen to start occurring at the values of ΔT as were predicted by the linear

analysis. Furthermore, all post-buckling paths are stable within the range of applied ΔT.

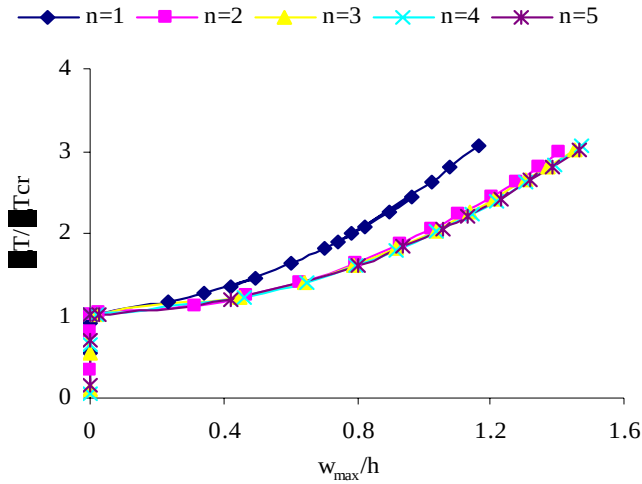

Figure 8.5. The thermal post-buckling of $[45/-45]_n$ composite plates (λ_1=55.3°C λ_2= 86.4°C λ_3=90.6 °C λ_4=92.1 °C λ_5=92.7 °C)

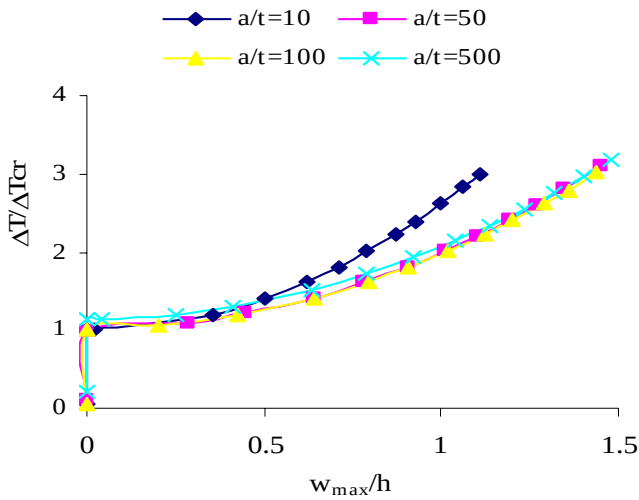

Figure 8.6. The thermal post-buckling of $[45/-45]_2$ composite plates with different side length to thickness ratios. (λ_{10}=6915.2°C λ_{50}= 453.0°C λ_{100}=115.7 °C λ_{500}=4.8 °C)

8.2.4. The effect of the boundary conditions

The three types of boundary conditions were applied on composite plates with the configuration of $[45/-45]_2$. Figure 8.7 shows that the lowest critical buckling (λ_{SS}=105.7°C) occurs when the SS boundary condition is used while the CC boundary condition gives the highest critical buckling (λ_{CC}=232.8°C). As in previous studies, buckling in all cases start to occur at the values of ΔT_{cr} as were predicted by the linear analysis. In addition, all post-buckling paths are stable within the range of applied ΔT.

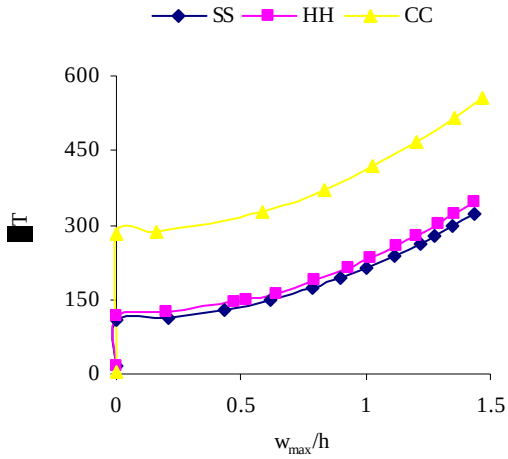

Figure 8.7. The Thermal Post-Buckling Of $[45/-45]_2$ Composite Plates With Different Boundary Condition.(λ_{SS}=105.7^{o}c λ_{HH}=115.7^{o}c λ_{CC}=232.77 ^{O}c)

8.2.5. The effect of the aspect ratios

In this study, the aspect ratios (a/b) are changed to see its effect on the thermal post-buckling behaviour of composite plates. It is noted in Figure 8.8 that as the aspect ratios are increased, the critical loads increased too. This is expected since as the aspect ratios are increased, the plates become less slender and the side where loading occurs is longer than the other side. Figure 8.8 also shows that in each case of a/b ratio, buckling starts to occur at Δ_{cr} as predicted by the linear analysis. It also shows that the ratios of $\frac{\Delta T}{\Delta T_{cr}}$ are higher for the same amount of lateral deflection if the aspect ratios are different from 1.

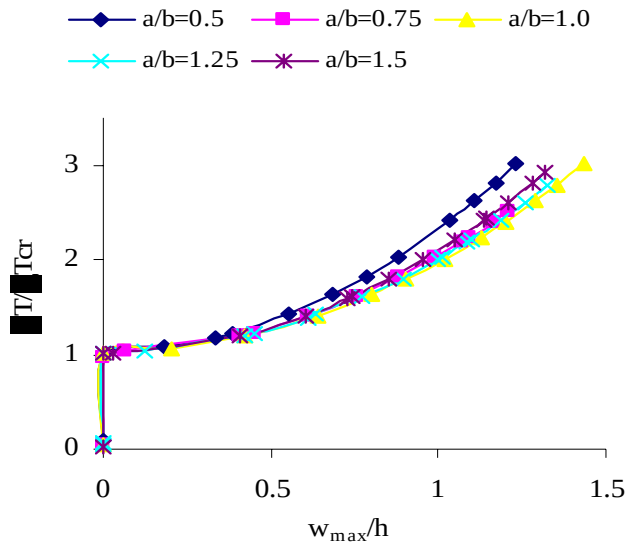

Figure 8.8. The Thermal Post-Buckling Of $[45/-45]_2$ Composite Plates With Different Aspect Ratios. ($\lambda_{0.5}$=60.3°c $\lambda_{0.75}$=87.1°c λ_1=105.7 °c, $\lambda_{1.25}$=144.4.1°c $\lambda_{1.5}$=173.8 °c)

8.2.6. The effect of the lamination angles

This study is conducted on the composites with configurations of $[\theta/-\theta]_2$ where θ can be 0°, 15°, 30°, 45°, 60°, 75° and 90°. The results for the θ of 60°, 75° and 90° are not shown in Figure 8.9 because they coincided with the curves for the θs of 30°, 15° and 0° respectively.

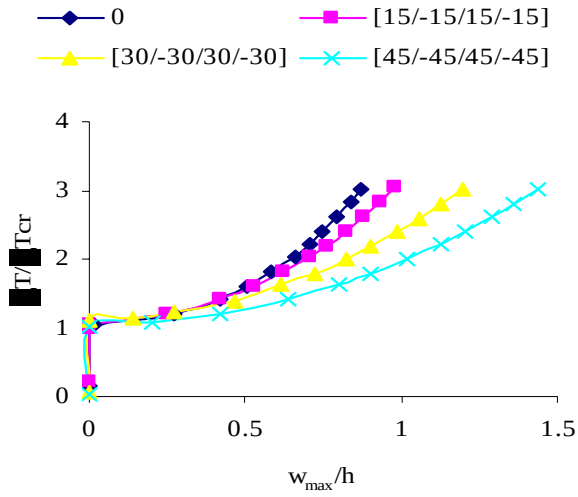

Figure 8.9. The thermal post-buckling of $[45/-45]_2$ composite plates for different boundary conditions. (λ_1=68.2°C λ_2=71.4°C λ_3=115.7 °C)

The graphs in Figure 8.9 shows that even though the $[45/-45]_2$ configuration gives the highest critical buckling (λ_3=115.7 °C), its ratio of $\frac{\Delta T}{\Delta T_{cr}}$ is the lowest ratios compared to other configurations for the same value of lateral displacements.

REFERENCES

[1] L. Librescu, W. Lin, M.P. Nemeth, and J.H. Starnes.1994. Effect of Tangential Edge Constraints On The Post-Buckling Behaviour of Flat And Curved Panels Subjected To Thermal And Mechanical Load. : Buckling And Post-Buckling of Composite Structures," *ASME AD*, vol. 41 / *PVP*, vol. 293: 115-133.

[2] M.R. Prabhu, and R. Dhanaraj. 1994. Thermal Buckling of Laminated Composite Plates, *Computer and structures*, vol. 53, no. 5:1193– 1204.

[3] C.A. Shankara and N.G.R. Iyengar. 1993. Finite Element Model for The Thermo-Mechanical Buckling Analysis of Composite Plates, *Composite Material Technology: American Society of Mechanical Engineers, Petroleum Division (Publication) PD*, vol. 53: 293-301.

[4] W.J. Chen, P.D. Lin, and L.W. Chen. 1991. Thermal Buckling Behaviour of Thick Composite Laminated Plates Under Non-Uniform Temperature Distribution, *Computer and structures,* vol. 41, no. 4: 637– 645.

[5] G. Singh, G.V. Rao, and N. G. R. Iyengar. 1993. Thermal Post-Buckling Behaviour of Laminated Plates, *AIAA Journals*, vol. 59: 1336– 1338.

[6] R.C. Averill and J.N. Reddy. 1993. Thermo-Mechanically Post-Buckling Analysis of Laminated Composite Shells, in *Proc. 1993 34th AIAA/ASME/ASCE /AHS/ASC Structures, Structural dynamics and Materials conference, AIAA-93-1337-CP* : 351-360.

[7] V.S. Thankam, G. Singh, G.V. Rao, and A. K. Rath. 2003. Thermal Post-Buckling Behaviour of Laminated Plates Using A Shear-Flexible Element Based on Coupled-Displacement Field, *Composite Structures*, vol. 59:351– 359.

[8] J.N. Reddy, *Mechanics of Composite Plates and Shells: Theory and Analysis,* 2nd Edition, New York: CRC Press, 2002.